# Comparison of surface-enhanced Raman scattering on graphene oxide, reduced graphene oxide and graphene surfaces

Huanping Yang [a,c], Hailong Hu [a], Zhenhua Ni [b], Chee Kok Poh [c], Chunxiao Cong [a], Jianyi Lin [c], Ting Yu [a,d,e,*]

[a] Division of Physics and Applied Physics, School of Physical and Mathematical Sciences, Nanyang Technological University, 637371 Singapore, Singapore
[b] Department of Physics, Southeast University, 211189 Nanjing, China
[c] Institute of Chemical and Engineering Sciences, A*STAR, 1 Pesek Road, Jurong Island, 627833 Singapore, Singapore
[d] Department of Physics, Faculty of Science, National University of Singapore, 117542 Singapore, Singapore
[e] Graphene Research Centre, National University of Singapore, 2 Science Drive 3, 117542 Singapore, Singapore

## ARTICLE INFO

## ABSTRACT

To explore the role of the interaction between the adsorbed molecules and substrates for the charge transfer (CT) induced Raman enhancement, we systematically study the surface enhanced Raman scattering (SERS) on graphene, graphene oxide (GO) and reduced graphene oxide (r-GO) using rhodamine 6G (R6G) as the probe molecule. The Raman spectra of R6G molecules deposited on these three SERS substrates show remarkable difference in spectral features due to the different enhancement contributions from the local chemical groups and the global $\pi$-conjugation network of the substrates. What is more surprising is that for 1–4 layers graphene-based materials, the Raman signals of R6G on GO are found to increase intensity with the number of GO layers, while the Raman signals of R6G on different graphene/r-GO layers show inverse trends due to dominant $\pi$–$\pi$ stacking mechanism. Our results provide a comprehensive understanding of the influence of local chemical groups and the global $\pi$-conjugation network on the SERS enhancements. In addition to high reproducibility, low cost, and good biocompatibility of GO, the rich chemical structures and the absence of electromagnetic enhancement make it an excellent choice as a tunable substrate to study the chemical enhancement resulting from the adsorbent–substrate interaction.

## 1. Introduction

Surface-enhanced Raman scattering (SERS) is one of the most important and powerful techniques to probe the chemical interaction between the adsorbing molecules and the surface of some metals, which are capable of amplifying the Raman signals of adsorbing molecules by 6–10 orders of magnitude [1–4]. It is well-known that there are two main contributions for this huge enhancement, namely, electromagnetic (EM) and chemical charge transfer (CT) enhancements. The latter one can offer more information about the adsorbate and adsorbent molecules, in particular, the adsorption orientation

---

[5,6]. However, these two inseparable mechanisms are usually concomitant in practice, with the EM enhancement playing dominate role. Hence, a SERS substrate without EM enhancement is highly desirable for the in-depth study on the CT effect.

Recently, few layers graphene has been demonstrated as an active SERS substrate which can drastically quench the fluorescence background of rhodamine 6G (R6G) [7–9] and enhance the Raman signal. Significantly, such enhancement by graphene substrates is considered as the consequence of CT between R6G and graphene, with no contribution from EM. These successes provide a direct and convincible way to understand the exact role of CT without the interference of EM. The different layers of graphene oxide (GO) and reduced graphene oxide (r-GO) are derivatives of graphene at different oxidation degrees. The active oxygen sites of GO and r-GO have been shown to notably enhance the binding between graphene and adsorbates (metal/molecule) [10,11]. Hence it is expected that GO, r-GO as well as graphene, all three graphene-based substrates can serve as excellent CT-only SERS substrates. Nevertheless, to our best knowledge, no systematic investigation of the SERS effect on these three substrates has been presented.

In this paper, R6G was used as a probe molecule to study and compare the SERS effects on graphene, GO and r-GO. Obvious enhancement of R6G Raman signals was observed on all the three substrates. Moreover selective enhancement of vibration modes was observable on GO, r-GO and graphene due to their difference in chemical groups and $\pi$-conjugation. The selectivity in signal enhancement of different spectral features may be attributed to the difference in the bonding and orientation of the adsorbed R6G molecules on these substrates. We also studied the effect of SERS on graphene layer number and observed opposite trends on GO vs. r-GO and graphene. With increasing the layer number of GO, the Raman signal of R6G increased, while both 1–4 layers graphene and r-GO substrates showed decreasing trend. This could be due to the different interference effect induced by increasing layers in graphene, r-GO and GO. These systematic spectral study and comparison could provide comprehensive good understanding of how SERS effects depend on the chemical interaction between molecules and graphene-based substrates.

## 2. Experimental

### 2.1. Chemicals

R6G, commercial expanded graphite (CEG), 98% $H_2SO_4$, 30% $H_2O_2$, 85% $H_3PO_4$ and $KMnO_4$ were purchased from Sigma–Aldrich without further purification.

### 2.2. Synthesis of GO

GO sheets were synthesized from CEG according to a modified Hummers method [12–15]. Typically 3 g of CEG was added into a 9:1 mixture of concentrated $H_2SO_4/H_3PO_4$ (360:40 mL) in a flask, which was immersed in an ice bath. Afterwards, 15 g

of $KMnO_4$ was slowly added to the solution. Meanwhile, the temperature of the mixed solution was maintained below 20 °C for 2 h to avoid overheating and explosion. The mixture was stirred for 5 days. Then, 10 mL of 30% $H_2O_2$ was added into the solution in order to completely react with the remaining $KMnO_4$, resulting in a bright yellow solution. Finally, the mixture was washed with distilled water until the pH of the solution was approximately 5. GO powder was obtained after freeze drying of the suspension.

### 2.3. Preparation of GO thin-film

Si wafer with 300 nm $SiO_2$ ($SiO_2$/Si) capping layer was used as the substrate of GO thin film. The $SiO_2$/Si substrates were cleaned in piranha solution [16] (a 3:1 mixture of concentrated 98% $H_2SO_4$ and 30% $H_2O_2$) at 100 °C for 1 h. The substrate surface became hydrophilic after the piranha treatment. GO films were deposited onto the $SiO_2$/Si substrates by dip-coating method.

### 2.4. Preparation of r-GO thin-film

R-GO film was produced by heating the as-prepared GO thin-film in a 1:5 $H_2$/Ar stream at 400 °C in a tube furnace for 2 h.

### 2.5. Preparation of graphene

Graphene was prepared using micromechanical exfoliation of HOPG, which was showed in Supporting information.

### 2.6. Preparation of SERS samples

R6G, a common probe molecule in SERS experiments, was used to verify the SERS effect of these three substrates. In a typical preparation, the graphene-based substrate, i.e. as-prepared GO thin-film, r-GO thin-film or graphene was first soaked in a $10^{-5}$ M R6G solution for 1 h, then washed with distilled water to remove those physically adsorbed molecules, and then dried in air.

### 2.7. Raman measurements

Raman spectra were recorded on the WITEC CRM200 Raman system using a 600 lines/mm grating and a 100× objective lens (NA = 0.95). Nd: YAG green laser with 532 nm wavelength was used to excite Raman signal with the low power of 0.1 mW. An integration time of 3 s was used in the measurements to reduce the heating effect induced by laser. The 2D Raman images were obtained by moving a piezo-stage with 100 nm step size. The ScanCtrl Spectroscopy Plus software (WITec GmbH, Germany) controlled the stage movement and recorded the data point by point. WITec Project software can also perform the analysis of Raman spectra and images.

### 2.8. X-ray photoelectron measurement

X-ray photoelectron spectroscopy (XPS) measurement was carried out on a Thermo Scientific ESCALAB 250.

## 3. Results and discussion

### 3.1. SERS of single layer GO, single layer r-GO and SLG

#### 3.1.1. Selective enhancement of vibrational Raman modes

The typical Raman spectra of R6G molecules adsorbed on single layer GO, single layer r-GO and single layer graphene (SLG) are shown in Fig. 1a, c, and e, respectively. All the three spectra show strong SERS peaks [17,18] with low fluorescence background. The prominent quenching of R6G fluorescence in these spectra is due to the absence of electromagnetic (EM) effect while the strong Raman signals are attributed to CT between the molecules and substrates, indicating the existence of strong chemical interaction. Importantly, the Raman spectra obtained from SLG, single layer GO and single layer r-GO exhibit distinguishable spectral features, namely, selective enhancement of Raman modes on different surfaces. Three bands characteristic of R6G, i.e. P1, P2 and P3 are observed in all the three spectra. P1 at $612\ cm^{-1}$ and P2 at $774\ cm^{-1}$ can be assigned to in-plane and out-of-plane bending motions of the carbon and hydrogen atoms of the xanthenes skeleton, respectively while the bands observed at $1648\ cm^{-1}$ (labelled as P3) is attributed to an aromatic stretching vibration mode. The positions of P1, P2 and P3 agree well to those reported for R6G on Ag nanoparticles [5,17] or in ethanol solution [19] though their relative intensity varies on the three graphene-based surfaces. The strongest peak remains as P3 on SLG (see Fig. 1e), which implies that
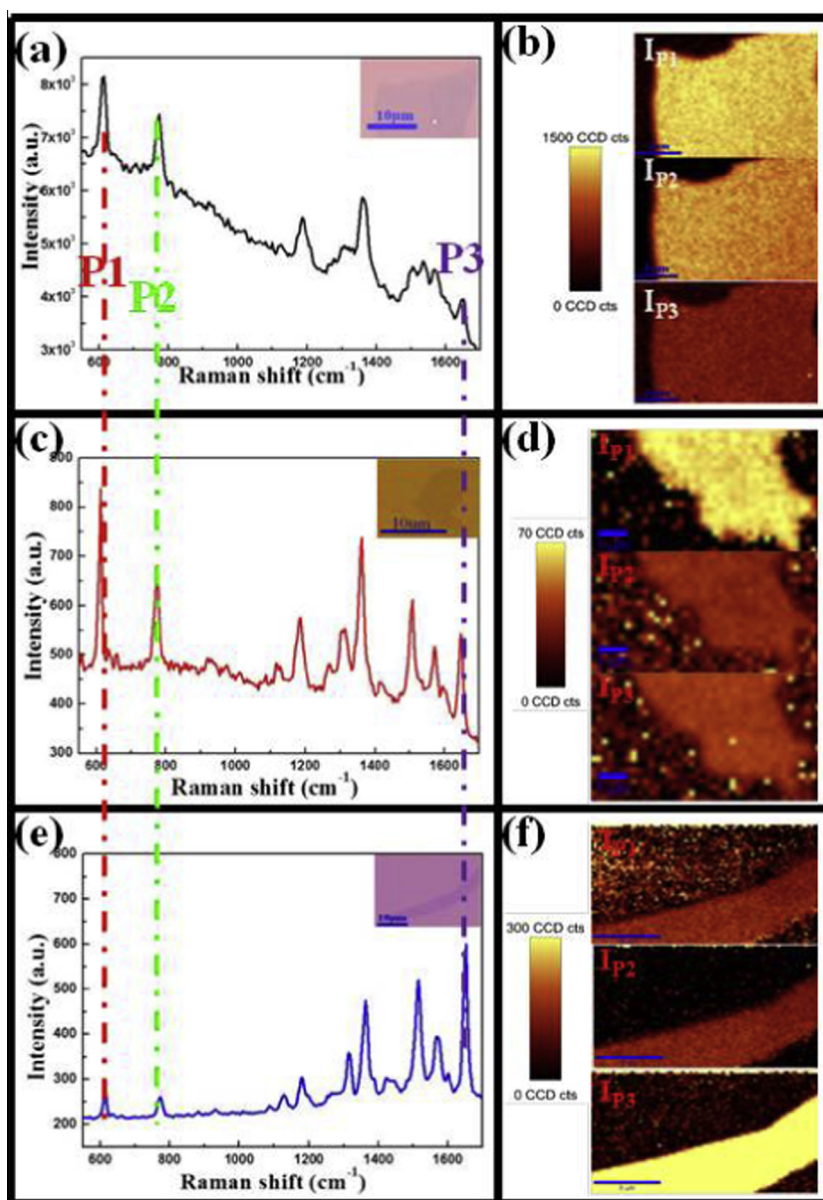


Fig. 1 – Typical Raman spectra of R6G on three different substrates, i.e. single layer GO (a and b), single layer r-GO (c and d) and single layer graphene (SLG) (e and f), all showing three peaks P1, P2 and P3, which are characteristic of R6G. The inset images are the optical images of these three samples. The corresponding Raman images of $I_{P1}$ (b, d and f-top), $I_{P2}$ (b, d and f-middle), $I_{P3}$ (b, d and f-bottom) are plotted alongside the Raman spectra on the three graphene-based surfaces.
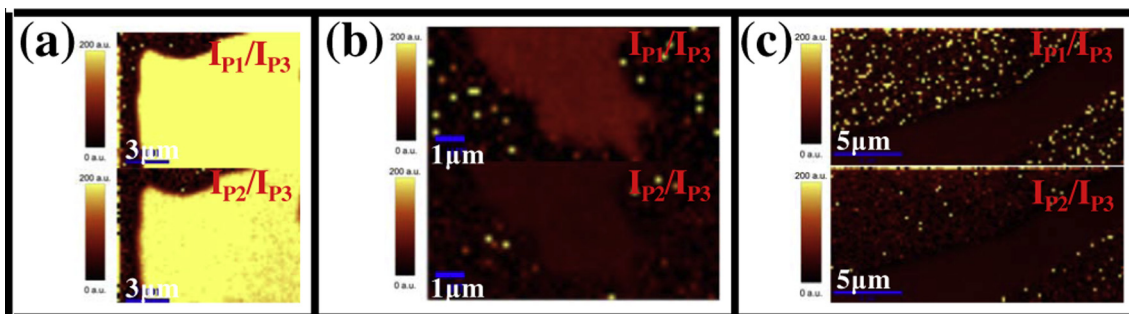
**Fig. 2 – Images of relative intensities ratios of selected P1, P2 and P3 Raman peaks of R6G on single layer GO (a), single layer r-GO (b) and SLG (c), respectively. Both $I_{P1}/I_{P3}$ (top) and $I_{p2}/I_{P3}$ (bottom) are the strongest on single layer GO and weakest on SLG (c-top).**
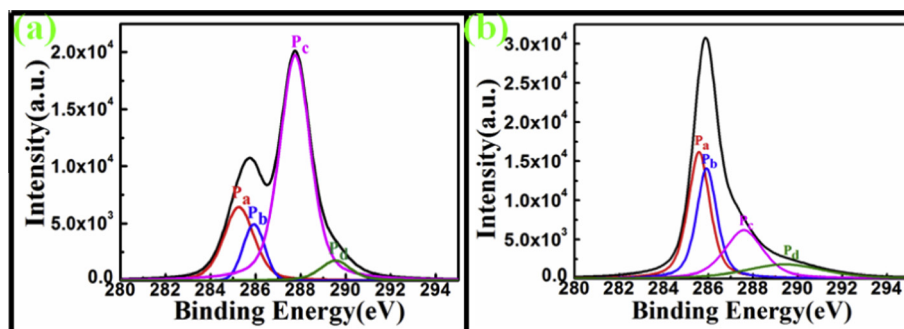


**Fig. 3 – Typical C1s XPS spectra of (a) the different layers of GO and (b) the different layers of r-GO. The spectra were fitted into four components Pa, Pb, Pc and Pd. The latter two peaks reflect the contributions from oxygen-bonded carbon species.**

the R6G molecules align their long axis along the graphene surface and interact with the SLG through the aromatic rings. The intensity of the P3 peak for single layer GO (see Fig. 1a) is much lower than P1 and P2 peaks (Fig. 1a), indicating that the aromatic rings of R6G are not parallel to the surface of single layer GO or the R6G aromatic rings and the single layer GO aromatic rings are separated by chemical groups. As for single layer r-GO the P3 peak intensity (Fig. 1c) is low but is relatively enhanced compared to that of single layer GO due to the recovery of the graphene structure. The relative intensity of these three peaks is P1 ≈ P2 > P3 for single layer GO; P1 > P2 ≈ P3 for single layer r-GO; and P1 ≈ P2 ≪ P3 for SLG. The correlated Raman mappings plotted based on the intensities of P1, P2 and P3 peaks are displayed in Fig. 1b, d and f, respectively.

To project the variation of the relative peak intensity on the three graphene-based surfaces, the images of $I_{P1}/I_{P3}$ and $I_{p2}/I_{P3}$ are plotted in Fig. 2. It becomes obvious that P1/P3 and P2/P3 in Fig. 2b for single layer r-GO are significantly lower than those of single layer GO in Fig. 2a.

The significant spectral differences in the obtained SERS spectra of R6G on these three SERS substrates could be attributed to the variation in adsorption bonding and molecular orientation. Most of the aromatic dye molecules such as R6G are found to lie parallel to the surface of graphene [7,20,21]. For the graphene substrate, the long axis of the R6G molecules should be approximately parallel to the layer of graphene due to strong π-π stacking, which induces charge transfer (CT) between the R6G and graphene and is responsi-

ble for the strong Raman signal enhancement and the quenching of fluorescence [7,20]. P1 and P2 are weak for SLG in Fig. 1e whereas they are relatively strong for GO as shown in Fig. 2a. Therefore, there most likely exists an additional enhancement mechanism for the different layers of GO and r-GO substrates besides the π–π stacking interaction. Yu et al. [11] reported that mildly reduced graphene oxide (MR-GO) nanosheets significantly increased the Raman signal of Rhodamine B (RhB) molecules due to the presence of highly electronegative oxygen species. The species can introduce a strong local electric field around the adsorbed molecules, which is possibly responsible for the additional enhancement. To determine the species and concentrations of oxygen functional groups on the different layers of GO and r-GO, XPS measurements were performed.

### 3.1.2. XPS measurements

The XPS C 1s spectra of the different layers of GO and r-GO are shown in Fig. 3a and b, respectively. According to the previous theoretical and experimental studies [11,22,23], the C1s spectra were fitted to four components, i.e. the $sp^2$ carbon peak centred at 285 eV (labelled as $P_a$), $sp^3$ hybridized carbon at 286 eV (labelled as $P_b$), C-O peak at 287.2 eV (labelled as $P_c$), and COO peak at 288.8 eV (labelled as $P_d$) respectively. Based on first principle calculation results [22], $P_c$ is the consequence of epoxy, ether, hydroxyl, carbonyl, and carbonyl-edge groups, while $P_d$ originates from epoxy pairs, epoxy–hydroxy pairs, and carboxyl groups. The low intensity of the $sp^2$ peak (Pa in Fig. 3a) and high intensity Pc peak imply that the

as-prepared the different layers of GO was heavily oxidized. The C/O atomic ratio was approximately 1.8:1 for the as-prepared the different layers of GO. After reduction, this ratio substantially increased to 15.8:1, indicating that most of the oxygen-related groups on the different layers of GO were removed and the graphene-like framework was nearly recovered.

As shown in Fig. 3a and b, the intensity of $P_a$ and $P_d$ peaks in r-GO are nearly unchanged after the reduction; while, $P_c$ is greatly depressed and $P_b$ greatly enhanced. The latter two peaks have significant changes with opposite trends which are similar to the observations reported by Yu et al. [11]. Yu et al. proposed that this phenomenon could be responsible for the change in Raman signals. The functional groups corresponding to $P_c$ are responsible for the Raman enhancement in GO, and they have structures different from sp$^2$ bonding $P_b$. As the number of C–O groups that contributed to the $P_c$ peak decreased, the single layer r-GO substrate produced higher Raman enhancement and the R6G fluorescence was further suppressed compared to the single layer GO substrate. It is worth mentioning that the removal of the functional groups that contribute to $P_c$ will most likely result in the formation of structural domains with defects (i.e. C–C single bonds and topological defects) on the graphene basal planet. This change can contribute to an increase in the $P_b$ intensity. The conductivity of the different layers of r-GO substrate is increased and its fluorescence quenching effect is stronger compared to those of different layers of GO [11].

Since as-prepared the different layers of GO substrate is highly oxidized, oxygen functional groups are present on the basal plane of the different layers of GO and some carbon atoms in the basal plane are removed, which would slightly distort the π-conjugation. The oxygen-containing groups related to $P_c$ can generate a strong local dipole moment ($\mu_{loc}$), which can induce a significant local electric field ($E_{loc}$) under laser excitation ($E_o$). Furthermore, due to the large polarizability ($\alpha$) induced by the large π-conjugated domains, the different layers of GO has an additional local electric field. The interaction between the local electric field and the molecules can be expressed by the formula: $E_{loc} = E_o + f(\mu_{loc} + \alpha E_o)$, where $f$ is a geometry-related parameter [11]. The enhanced electric field can spontaneously lead to an orientation change in the R6G molecules on the different layers of GO surface, which would result in higher Raman signals for P1 and P2 than that of P3. Simultaneously, the Raman bands of R6G can be enhanced by a highly polarized electric field through coupling with the Raman polarizability tensors. Nevertheless, when reducing different layers of GO to r-GO, the local dipole moment and the polarizability of the different layers of r-GO will decrease due to the increments of $P_b$ component and the destruction of π-conjugation. The global polarized electric field of different layers of r-GO can still affect the orientation of the R6G on different layers of r-GO and result in strong Raman signal for P1 vibration mode. Therefore, the overall Raman enhancement of different layers of GO and different layers of r-GO result from both the π–π stacking interaction and the weak local electric field from the substrate [11,24].

### 3.1.3.    Effect of local electronegative oxygen species

To further investigate the effect of the local electronegative oxygen species on SERS, we performed a controllable experiment to adjust the amount of oxygen species through controlling the pH value of GO films prior to soaking into R6G solution. By pre-treating with NaOH or HCl solution, the GO films were expected to respectively cover with high or low concentration of negative oxygen species [25–27]. The corresponding SERS spectra obtained from the untreated and treated samples are shown in Fig. 4. P1 and P2 intensities are seen to increase from the bottom to top spectrum in Fig. 4, revealing obvious additional enhancements of P1 and P2 modes due to the increase of negative species. Such observations provided convincible evidence that the local electronegative oxygen species of different layers of GO could be a dominant contribution to Raman enhancement.

The electronegative oxygen species on GO and r-GO is similar with the halide salts on metal nanoparticles [28–31], which has been much discussed in the literature, and both the proposed mechanisms, including salt effect on electromagnetic or chemical enhancements. These authors concluded that adsorbed chloride ions locally modify the
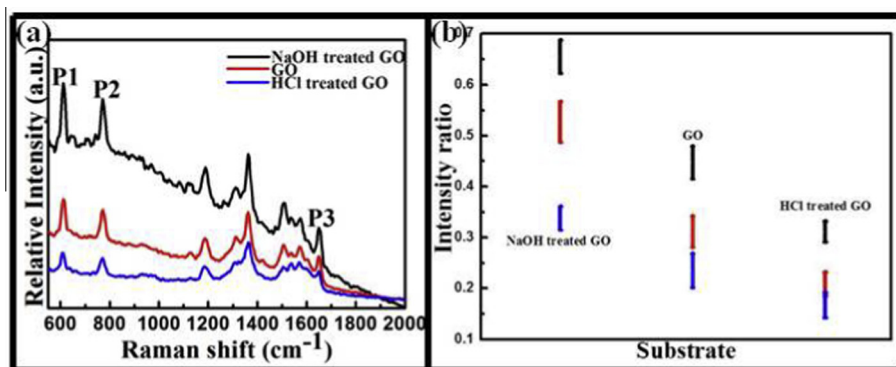


Fig. 4 – (a) Typical Raman spectra of the R6G on untreated (red), NaOH-treated (black) and HCl-treated (blue) single layer GO. It is known that the concentration of electronegative oxygen species is decreased in the order: NaOH-treated-GO > GO > HCl-treat-GO. (b) The intensity ratiao of P1, P2 and P3 with Si peak intensity on GO, NaOH-treated GO and HCl-treated GO (from left to right). (For interpretation of the references to colour in this figure legend, the reader is referred to the web version of this article.)
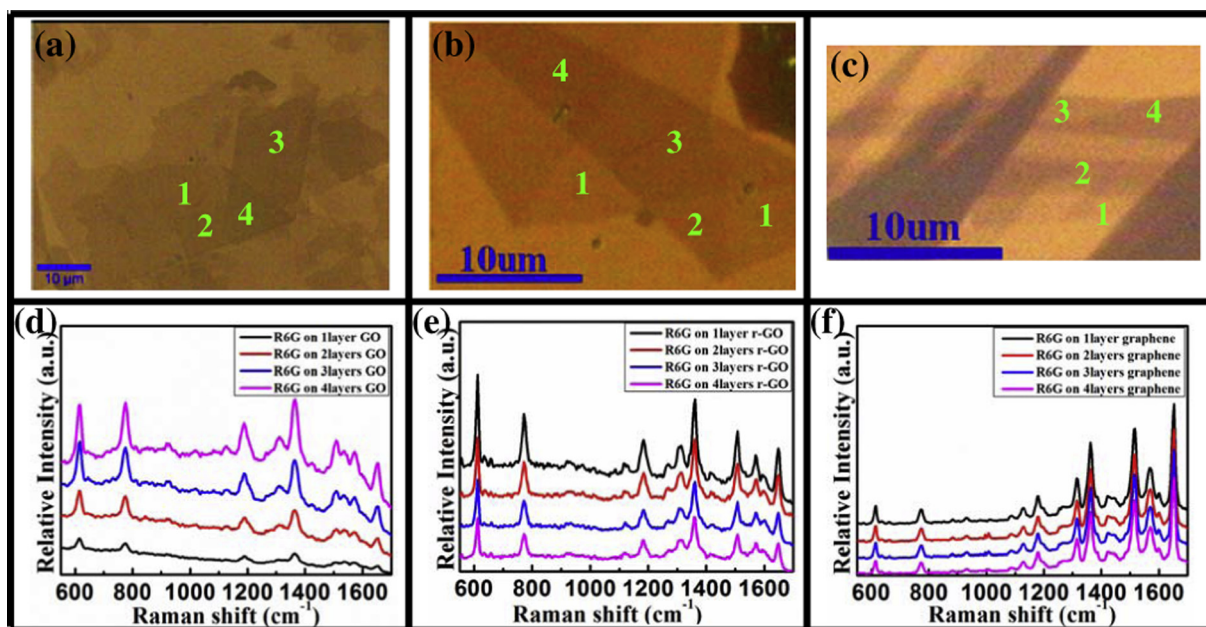
Fig. 5 – The optical images of 1–4 layered GO (a), r-GO (b) and graphene (c) (The number of layers of the GO, r-GO and graphene are labelled in the images), and the typical Raman spectra of the R6G adsorbed on 1–4 layered GO (d), r-GO (e) and graphene (f).
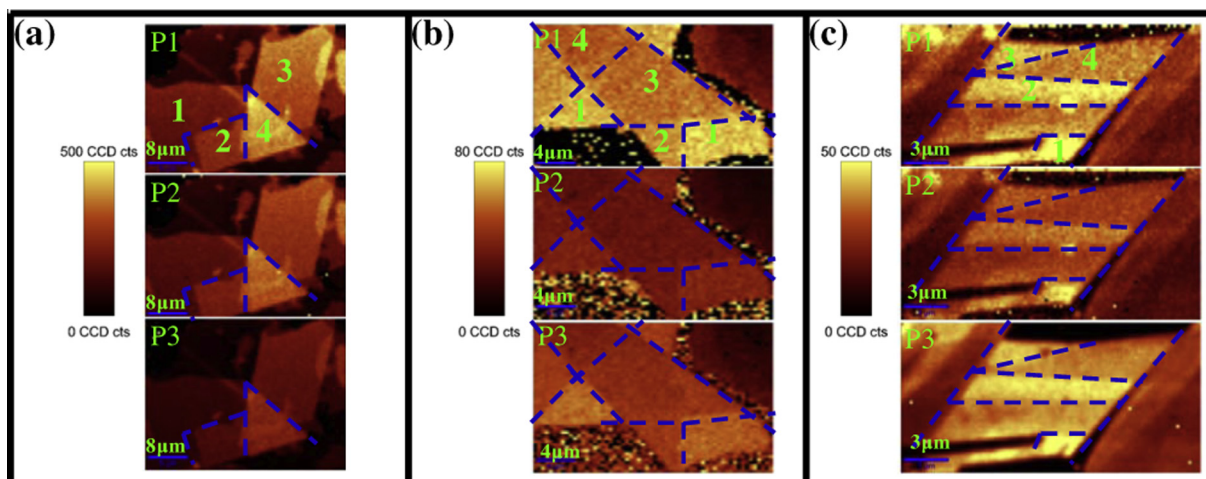


Fig. 6 – Typical Raman images of the R6G P1, P2 and P3 peaks respectively on 1–4 layered GO (a), r-GO (b) and graphene (c). (The number of layers of the GO, r-GO and graphene are labelled in the P1 images at the top image of a–c. The blue dotted lines show the borders between the regions of different numbers of layers). (For interpretation of the references to colour in this figure legend, the reader is referred to the web version of this article.)

surface electronic structure, and that such modification is accompanied by reorientation of adsorbed molecules in flat surface conformation. Denis et al. [5] reported that different vibrational bands of R6G responded differently to the introduction of NaCl. Specifically, the enhancement factor for 1365 and 1512 cm$^{-1}$ vibrational bands was 3.2, which is significantly larger than enhancement factors of 2.3 calculated using bands at 615 and 775 cm$^{-1}$. The spectral assignment of 1365 and 1512 cm$^{-1}$ bands as aromatic C–C stretching in-ring vibrational bands and band at 776 cm$^{-1}$ as C–H out-of-plane bend vibrations are consistent with suggested orienta-

tion changes of R6G molecules caused by coadsorption of Cl ions. Therefore, our observations of the relative vibrations bonds are consistent with suggested orientation changes of R6G molecules caused by the electronegative oxygen species on GO and r-GO.

### 3.2. Layer number effect

It is well-known that the electronic structures and properties of graphene, GO and r-GO are highly dependent upon the graphene layer number. Hence, we prepare 3 samples with
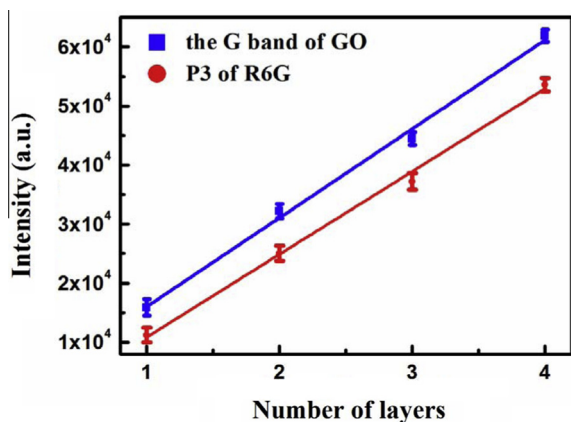
**Fig. 7 – The Raman intensity of the G-band of GO sheets (blue) and P3 peak (red) of R6G as a function of the number of layers of GO sheets. (For interpretation of the references to colour in this figure legend, the reader is referred to the web version of this article.)**

1–4 layers for each graphene-based sample as the SERS substrates for this study (see Fig. 5). The layer number of the samples was determined using contrast spectroscopy. From Fig. 5, it is noticed that the Raman spectra of R6G on the three SERS substrates show different thickness dependence: for 1–4 layers GO (Fig. 5a), monolayer < bilayer < trilayer < tetralayer; for 1–4 layers r-GO and graphene (Fig. 5b and c), monolayer > bilayer > trilayer > tetralayer. The investigation of SERS spectra from these three samples with different layers could get deeper insight into the chemical interactions between adsorbed molecules and substrates.

Fig. 6 displays the corresponding Raman mapping of P1, P2 and P3 on the above 3 sets of 1–4 layered samples, demonstrating high uniformity and reproducibility of these samples as SERS substrates.

In our previous work [32–34], the G band intensity dependency on the number of graphene or GO layers was successfully explained using Fresnel's equations, by considering the interference between the incident laser and scattered Raman signal in the graphene/GO layers. Similarly we can use Fresnel's equations to understand the layer number effect of SERS. In Fig. 7 the R6G P3 peak (P3) is plotted as the function of GO layer number.

It is interesting to note that the intensity of P3 increases with the number of layers, which is analogous with the tendency of the corresponding G peaks in different layers of GO. Therefore, The trend for the enhancement effect of GO with the number of layers could be explained by the interference effect. In the case of graphene, Ling et al. [20] reported that the interference effect induced by different numbers of graphene layers did not significantly contribute to the Raman intensity observed for the deposited molecules. The electrical conductivity of different layers of r-GO is recovered due to the restoration of the π-conjugation network, of which the value is approaching that of graphene. Thus, it is rationalized that different layers of r-GO shows a similar trend as different layers of graphene, and the interference effect induced by the

different numbers of layers for r-GO does not play a major role in the SERS enhancement of the adsorbed molecules.

## 4.    Conclusions

Based on the above studies, we conclude that the oxygenated groups and the π-conjugation on different layers of graphene, r-GO and GO substrates can significantly affect the bonding and orientation of the R6G adsorption, which results in the substrate-selective and the layer-number dependent enhancement of the Raman signals for the molecules on the three substrates. For R6G on graphene π–π stacking is the dominant CT mechanism for SERS and the Raman intensity decreases with increasing layer number. In contrast, the Raman signals of the molecules generally increase with increasing the number of the GO layers and oxygenated groups may play significant role in the SERS on GO surfaces. This is the first report of systematic comparison regarding the Raman enhancement of the molecules on the surface of different layers of graphene, r-GO and GO. As SERS substrates, different layers of GO and r-GO have many advantages over different layers of graphene such as easier preparation, lower cost, and better biocompatibility. Moreover, compared to different layers of r-GO and graphene, ultrathin (⩽4 layers) GO sheets result in a stronger Raman enhancement. This study provides a general understanding of the substrates effect on the bonding and orientation of the molecule adsorption, which will be beneficial for the study on the chemical enhancement mechanism regarding the interaction between the molecule and the substrates.

## Appendix A.    Supplementary material

Supplementary data associated with this article can be found, in the online version, at http://dx.doi.org/10.1016/j.carbon.2013.06.027.

REFERENCES

[1] Otto A, Mrozek I, Grabhorn H, Akemann W. Surface-enhanced Raman-scattering. J Phys-Condes Matter 1992;4(5):1143–212.
[2] Moskovits M. Surface-enhanced spectroscopy. Rev Mod Phys 1985;57(3):783–826.
[3] Schatz GC. Theoretical-studies of surface enhanced Raman-scattering. Acc Chem Res 1984;17(10):370–6.
[4] Campion A, Kambhampati P. Surface-enhanced Raman scattering. Chem Soc Rev 1998;27(4):241–50.
[5] Pristinski D, Tan SL, Erol M, Du H, Sukhishvili S. In situ SERS study of Rhodamine 6G adsorbed on individually immobilized Ag nanoparticles. J Raman Spectrosc 2006;37(7):762–70.

[6] Nie SM, Emery SR. Probing single molecules and single nanoparticles by surface-enhanced Raman scattering. Science 1997;275(5303):1102–6.

[7] Ling X, Zhang J. First-layer effect in graphene-enhanced Raman scattering. Small 2010;6(18):2020–5.

[8] Ling X, Zhang J. Interference phenomenon in graphene-enhanced Raman scattering. J Phys Chem C 2011;115(6):2835–40.

[9] Xie LM, Ling X, Fang Y, Zhang J, Liu ZF. Graphene as a substrate to suppress fluorescence in resonance Raman spectroscopy. J Am Chem Soc 2009;131(29):9890–1.

[10] Goncalves G, Marques P, Granadeiro CM, Nogueira HIS, Singh MK, Gracio J. Surface modification of graphene nanosheets with gold nanoparticles: the role of oxygen moieties at graphene surface on gold nucleation and growth. Chem Mater 2009;21(20):4796–802.

[11] Yu XX, Cai HB, Zhang WH, Li XJ, Pan N, Luo Y, et al. Tuning chemical enhancement of SERS by controlling the chemical reduction of graphene oxide nanosheets. ACS Nano 2011;5(2):952–8.

[12] Hernandez Y, Nicolosi V, Lotya M, Blighe FM, Sun ZY, De S, et al. High-yield production of graphene by liquid-phase exfoliation of graphite. Nat Nanotechnol 2008;3(9):563–8.

[13] Hummers WS, Offeman RE. Preparation of graphitic oxide. J Am Chem Soc 1958;80(6). 1339-1339.

[14] Xu YX, Bai H, Lu GW, Li C, Shi GQ. Flexible graphene films via the filtration of water-soluble noncovalent functionalized graphene sheets. J Am Chem Soc 2008;130(18):5856–7.

[15] Yang HP, Jiang J, Zhou WW, Lai LL, Xi LF, Lam YM, et al. Influences of graphene oxide support on the electrochemical performances of graphene oxide–$MnO_2$ nanocomposites. Nanoscal Res Lett 2011;6:531–8.

[16] Su CY, Xu YP, Zhang WJ, Zhao JW, Tang XH, Tsai CH, et al. Electrical and spectroscopic characterizations of ultra-large reduced graphene oxide monolayers. Chem Mater 2009;21(23):5674–80.

[17] Hildebrandt P, Stockburger M. Surface-enhanced resonance Raman-spectroscopy of rhodamine-6G adsorbed on colloidal silver. J Phys Chem 1984;88(24):5935–44.

[18] Watanabe H, Hayazawa N, Inouye Y, Kawata S. DFT vibrational calculations of Rhodamine 6G adsorbed on silver: analysis of tip-enhanced Raman spectroscopy. J Phys Chem B 2005;109(11):5012–20.

[19] Liu SS, Wan SB, Chen MD, Sun MT. Theoretical study on SERRS of rhodamine 6G adsorbed on $Ag_2$ cluster: chemical mechanism via intermolecular or intramolecular charge transfer. J Raman Spectrosc 2008;39(9):1170–7.

[20] Ling X, Xie LM, Fang Y, Xu H, Zhang HL, Kong J, et al. Can graphene be used as a substrate for Raman enhancement? Nano Lett 2010;10(2):553–61.

[21] Humbert C, Volcke C, Sartenaer Y, Peremans A, Thiry PA, Dreesen L. Molecular conformation and electronic properties of protoporphyrin-IX self-assembled monolayers adsorbed on a Pt(111) surface. Surf Sci 2006;600(18):3702–9.

[22] Zhang WH, Carravetta V, Li ZY, Luo Y, Yang JL. Oxidation states of graphene: insights from computational spectroscopy. J Chem Phys 2009;131(24). 244505-1-244505-6.

[23] Tung VC, Allen MJ, Yang Y, Kaner RB. High-throughput solution processing of large-scale graphene. Nat Nanotechnol 2009;4(1):25–9.

[24] Yang XY, Zhang XY, Liu ZF, Ma YF, Huang Y, Chen Y. High-efficiency loading and controlled release of doxorubicin hydrochloride on graphene oxide. J Phys Chem C 2008;112(45):17554–8.

[25] Li D, Muller MB, Gilje S, Kaner RB, Wallace GG. Processable aqueous dispersions of graphene nanosheets. Nat Nanotechnol 2008;3(2):101–5.

[26] Pan DY, Zhang JC, Li Z, Wu MH. Hydrothermal route for cutting graphene sheets into blue-luminescent graphene quantum dots. Adv Mater 2010;22(6):734–8.

[27] Kim J, Cote LJ, Kim F, Yuan W, Shull KR, Huang JX. Graphene oxide sheets at interfaces. J Am Chem Soc 2010;132(23):8180–6.

[28] Michaels AM, Nirmal M, Brus LE. Surface enhanced Raman spectroscopy of individual rhodamine 6G molecules on large Ag nanocrystals. J Am Chem Soc 1999;121(43):9932–9.

[29] Doering WE, Nie SM. Single-molecule and single-nanoparticle SERS: examining the roles of surface active sites and chemical enhancement. J Phys Chem B 2002;106(2):311–7.

[30] Grochala W, Kudelski A, Bukowska J. Anion-induced charge-transfer enhancement in SEES and SERRS spectra of rhodamine 6G on a silver electrode: how important is it? J Raman Spectrosc 1998;29(8):681–5.

[31] Jeong DH, Jang NH, Suh JS, Moskovits M. Photodecomposition of diazanaphthalenes adsorbed on silver colloid surfaces. J Phys Chem B 2000;104(15):3594–600.

[32] Ni ZH, Wang HM, Kasim J, Fan HM, Yu T, Wu YH, et al. Graphene thickness determination using reflection and contrast spectroscopy. Nano Lett 2007;7(9):2758–63.

[33] Yang HP, Hu HL, Wang YY, Cong CX, Yan JX, Shen ZX, et al. Rapid and non-destructive identification of graphene oxide thickness using white light contrast spectroscopy. Carbon 2013;52:528–34.

[34] Wang YY, Ni ZH, Shen ZX, Wang HM, Wu YH. Interference enhancement of Raman signal of graphene. Appl Phys Lett 2008;92(4). 043121-1-043121-3.